(NP,IT) International Symposium on the Physics and Chemistry of Finite Systems:
From Clusters to Crystals, Richmond, VA October 8-12, 1991 (proceedings)

MELTING OF NICKEL CLUSTERS

I. L. GARZÓN[1] AND J. JELLINEK[2]

[1]*Instituto de Física, Universidad Nacional Autónoma de México, Apartado Postal 2681, 22800 Ensenada, Baja California, México*
[2]*Chemistry Division, Argonne National Laboratory, Argonne, Illinois 60439 USA*

ABSTRACT. The meltinglike phenomenon in Ni_n, n = 19,20,55, clusters is studied using microcanonical molecular dynamics simulations. The interaction between the atoms in the clusters is modelled by a size-dependent Gupta-like potential that incorporates many-body effects. The clusters display the "usual" stages in their meltinglike transition, which characterize also Lennard-Jones (e.g., noble gas) and ionic clusters. In addition, Ni_{20} passes through a so-called premelting stage found earlier also for Ni_{14}.

1. Introduction

Phase changes, especially the meltinglike phenomenon, is one of the challenging and ever more active areas of cluster and small particle research [1]. Until recently, the bulk of the theoretical work concentrated primarily on Van der Waals (Lennard-Jones) systems. Most of the experimental studies, however, were performed on metal microparticles [2]. Different microscopy techniques were utilized to detect the melting (or the solidification) transition and to characterize the size dependence of the melting temperature of metal particles in the micrometer and nanometer size ranges. Only in a few theoretical studies has the phenomenon of a solid-to-liquid like transition in small metal clusters been considered. Sawada and Sugano [3] used a Gupta-like potential to characterize the meltinglike behavior of 6- and 7-atom transition metal clusters. They identified a so-called fluctuating state in the 6-atom cluster in which structural rearrangements can take place in a diffusionless manner. Ercolessi et al [4] employed the so-called "glue" potential to study the melting behavior of the Au_n, n = 219, 477, and 879. Surface melting as a precursor to complete melting has been found for n = 477 and 879. Surface melting in such a small cluster as Cu_{55} has also been detected in simulation studies of Cheng and Berry [5]. We have performed a molecular dynamics investigation of the meltinglike transition in 12- 13-, and 14-atom transition metal clusters [6] and 6-, 7-, and 13-atom gold clusters [7] using a size-dependent Gupta-like potential. For Ni_{13}, only a small reduction (~6%) in the melting temperature, as compared to the bulk value, is predicted. The corresponding reduction in the melting temperature of Au_{13} is estimated at ~50%. A novel intermediate stage in the meltinglike transition in clusters, which we called "premelting" [6] and which is, in general, different from the so-called "coexistence" [1], has been found for Ni_{14}. Both the qualitative and the quantitative features of the nickel clusters mentioned have been reproduced recently using an embedded-atom potential [8].

Here we report results on the meltinglike behavior of Ni_n, n = 19, 20, 55, derived from the size-dependent Gupta-like potential. The theoretical background and the computational

procedure are sketched in the next section. The results are presented and discussed in section 3. A summary is given in section 4.

2. Theoretical Background and Computational Procedure

The dynamical behavior of the clusters at different fixed total energies was obtained by solving numerically Newton's equations of motion for all the degrees of freedom. The forces acting on the atoms were calculated from a size-dependent many-body Gupta-like interaction potential, which is written in reduced units of the potential energy V^* and interatomic distances r_{ij}^* [6] as

$$V^* = \frac{1}{2} \sum_{j=1}^{n} \left\{ A \sum_{i=1}^{n} \exp(-p(r_{ij}^*-1)) - \left[\sum_{i=1}^{n} \exp(-2q(r_{ij}^*-1)) \right]^{1/2} \right\} \qquad (1)$$

The values of the parameters for nickel are: A = 0.101036, p=9, q=3 [3,6]. The absolute potential energy V and distances r_{ij} are obtained from their corresponding reduced values V^* and r_{ij}^* using material- and size-dependent units of energy U_n and distance r_{on}: $V = V^* \cdot U_n$, $r_{ij} = r_{ij}^* \cdot r_{on}$ [6]. The clusters were prepared initially with zero total linear and angular momenta. The Verlet algorithm [9] was utilized to integrate the equations of motion. Trajectories of length of 10^5 - 10^6 steps, with a step size of $7.8 \cdot 10^{-16}$s, were generated on a grid of total energies (per atom) large enough to observe the solid-to-liquid like transition in each cluster. The total energy in the individual runs was conserved within 0.75%.

To detect and characterize the meltinglike transition, a variety of quantities was calculated along the trajectories. Of these we present in the next section the following: (1) Short-time (over 500 steps) average of the kinetic energy per atom as a function of time. The goal of this averaging is to attenuate the fluctuations in the kinetic energy caused by the vibrational motions. (2) Caloric curve, i.e., long-time (along the entire trajectory) average of the kinetic energy per atom as a function of the total energy per atom. (3) Root-mean-square (rms) bond length fluctuation δ,

$$\delta = \frac{2}{n(n-1)} \sum_{i<j}^{n} \frac{(\langle r_{ij}^2 \rangle - \langle r_{ij} \rangle^2)^{1/2}}{\langle r_{ij} \rangle} , \qquad (2)$$

as a function of temperature κT (in energy units),

$$\kappa T = \frac{2\langle E_\kappa \rangle}{3n-6} , \qquad (3)$$

where E_κ is the total kinetic energy of the atoms in a cluster, κ is the Boltzmann constant, and $\langle\ \rangle$ stands for the long-time average.

3. Results and Discussion

We have determined the minimum energy structures of the clusters performing numerical thermal quenching. The double icosahedron is the most stable geometry of Ni_{19} (V^* = -18.641). The most stable configuration of Ni_{20} (V^* = -19.646) is the 19-atom double

icosahedron with an additional atom placed over a threefold face between two fivefold rings. The most stable structure of Ni_{55} ($V^* = -57.400$) is a two-shell icosahedron.

Figure 1 displays the short-time averaged kinetic energy per atom as a function of time for different total energies per atom. As the total energy increases, the pattern of the graphs for Ni_{19} and Ni_{55} changes from an essentially constant, to moderately fluctuating but single-branched, to multi-branched, and eventually to highly fluctuating with no individual branches resolvable. This evolution of the pattern is similar to that observed in certain size Lennard-Jones and ionic clusters [1], as well as in Ni_{12} and Ni_{13} [6,8]. Graphs (a) correspond to low-energy rigid clusters, graphs (b) - to "softer" but still preserving their structure clusters, graphs (c) - to spontaneous isomerization transitions (the different branches represent different isomers), and graphs (d) - to high-energy "melted" or liquid-like clusters. The changes in the pattern for Ni_{20} are, however, different. First the short-time averaged kinetic energy converts from a nearly constant (a) to a two-branched (b), then again to a single-branched albeit with larger fluctuations (c), then to multi-branched (d), and eventually to strongly fluctuating with no separable branches (e). A similar evolution of the graphs with the total energy is characteristic also for Ni_{14} [6,8]. It has not, however, been found in 14- and 20-atom Lennard-Jones or ionic clusters. As in the case of Ni_{14}, the two-branched curve (b) corresponds to the "premelting" stage, which involves only a limited topological rearrangement in the vicinity of the additional to the double icosahedron "surface" atom. Graph (d) represents isomerization transitions involving the entire Ni_{20} cluster. Graph (c) corresponds to a stage that is intermediate between the premelting and the full blown isomerizations; the two-branched pattern of premelting is obscured by the fluctuations due to large-amplitude oscillations in the underlying Ni_{19}. The (a) and (e) graphs correspond to the solidlike and liquidlike forms, respectively, of the Ni_{20} cluster.

In Figure 2, the caloric curves for the three clusters are shown. The meltinglike transition is associated with the variations in the slope of the curves. These variations are much larger in complete shell icosahedra Ni_{19} and Ni_{55} than in Ni_{20}.

Finally, the rms bond length fluctuations δ as a function of κT are depicted in Figure 3. The sharp rise in δ for Ni_{19} and Ni_{55} signifies the meltinglike transition in these clusters (cf. the Lindemann criterion [10]). The graph for Ni_{20} displays two abrupt changes: the first one, at lower temperature, corresponds to premelting, while the second one, at higher temperature, - to complete melting. To find the absolute temperatures at which the δ's change sharply, one has to convert the corresponding κT values from reduced to absolute units. The needed for this values of U_n (see section 2) were obtained in accordance with $U_n = V_n/V_n^*$; the calculated in the framework of an embedded-atom approach energies of the most stable structures [11] were used as V_n and the listed above corresponding energies in reduced units as V_n^* (incidentally, by comparing the characteristic distances in these structures in absolute and reduced units of length, one obtains the values of r_{on}). The magnitudes of $U_{19} = 3.380$ eV and $U_{55} = 3.537$ eV put the melting temperature (as specified by the value $\delta = 0.18$) of the Ni_{19} and the Ni_{55} clusters at ~1080K and ~1300K, respectively. We have not determined the exact value of U_{20}, but estimated it to be very

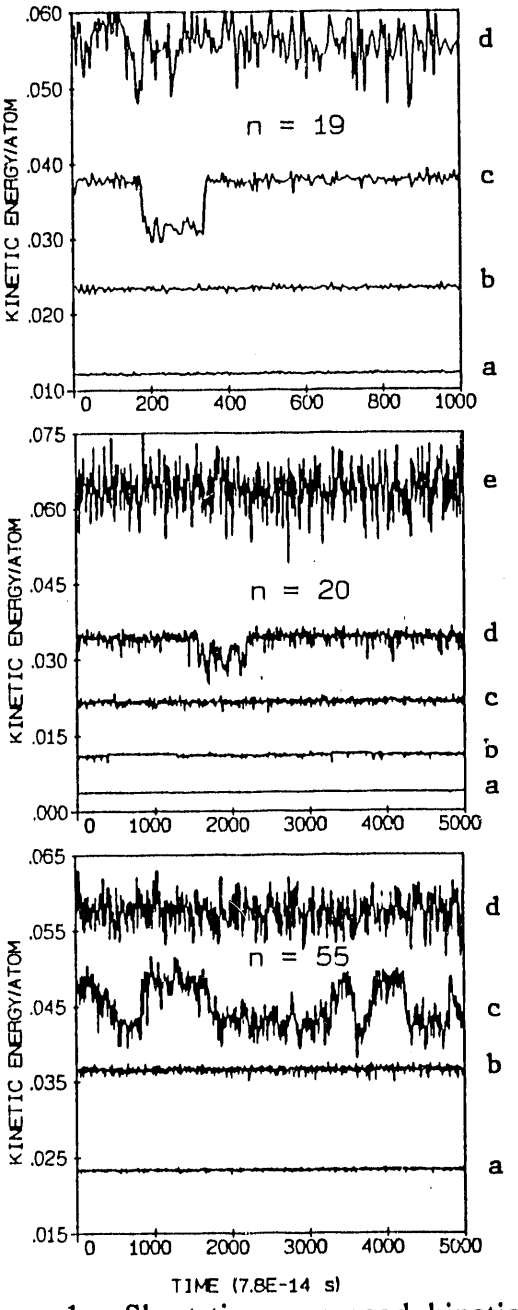

Figure 1. Short-time averaged kinetic energies per atom (in reduced units) as a function of time. The total energies per atom (in reduced units) are: n=19: a) -0.963, b) -0.945, c) -0.923, d), -0.884; n -20: a) -0.977, b) -0.965, c) -0.949, d) -0.929, e) -0.873; n = 55: a) -1.008, b) -0.987, c) -0.966, d) -0.941.

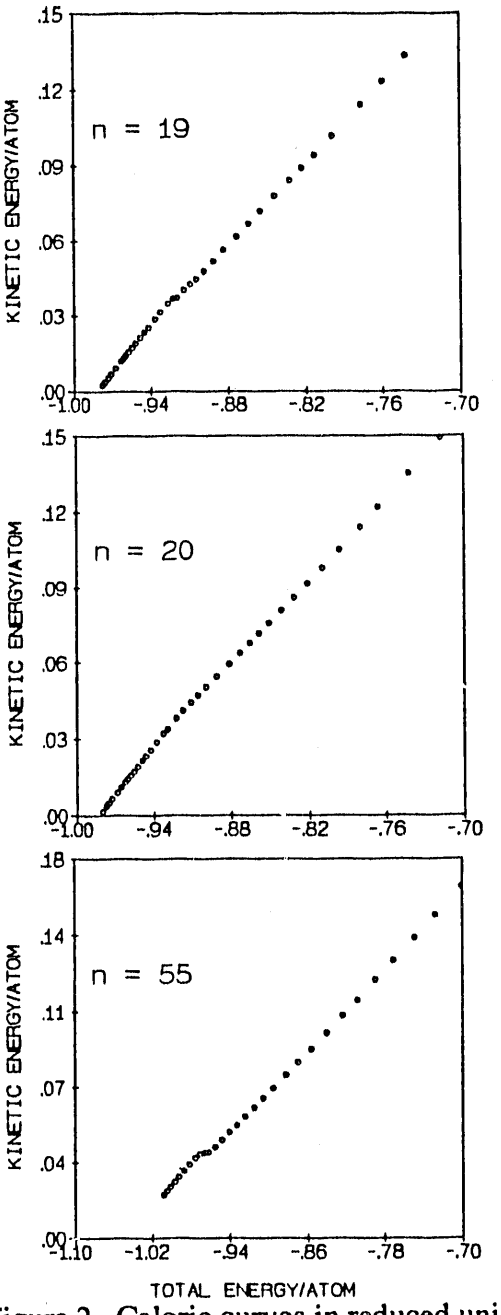

Figure 2. Caloric curves in reduced units of energy. The full circles correspond to total energies per atom considered in Fig. 1.

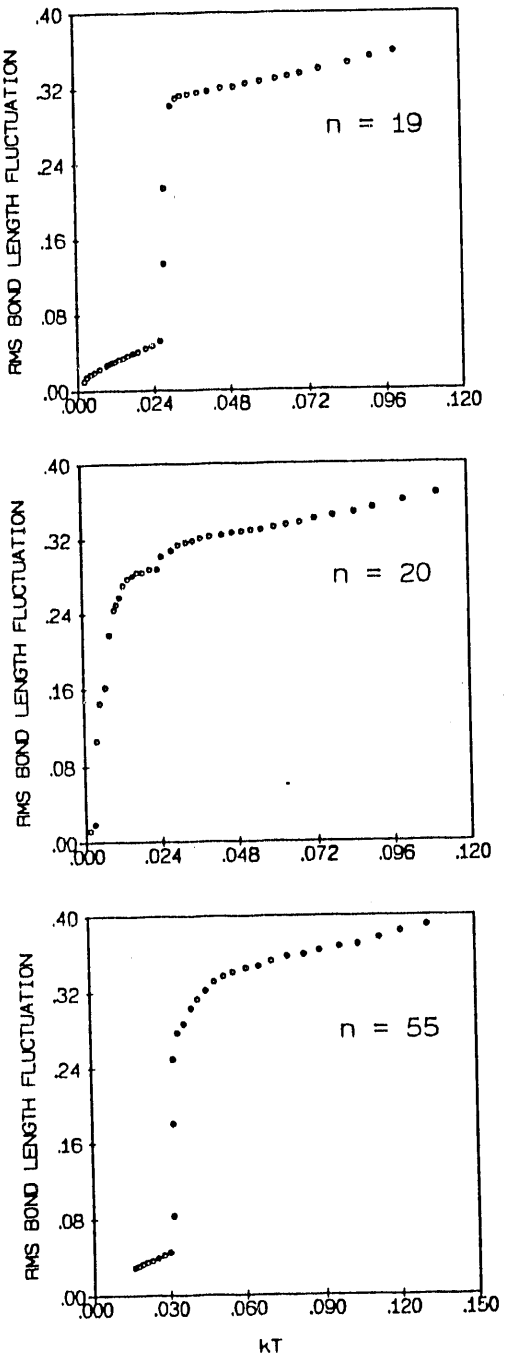

Figure 3. Rms bond-length fluctuations as a function of κT (in reduced units). The full circles correspond to total energies per atom considered in Figure 1.

close to that of U_{19}, although slightly smaller. This puts the premelting and melting temperatures of Ni_{20} at ~210±50K and ~930±50K, respectively.

4. Summary

A brief discussion of the meltinglike behavior of Ni_n, n=19,20,55, clusters described by a size-dependent Gupta-like potential has been presented. As the internal energy of the clusters is increased, they undergo a solid-to-liquid like transition which, similar to the case of Van der Waals and ionic clusters, includes an isomerization ("coexistence") stage. The Ni_{20} cluster exhibits also a low-temperature premelting state similar to that found earlier for Ni_{14}. It appears that the premelting phenomenon is characteristic of clusters with complete shell icosahedral geometries plus one atom, provided the potential describing the interaction between the atoms incorporates many-body effects. It is of interest to test this proposition on Ni_{56}, Ni_{148},... clusters.

Acknowledgments

This work was supported by DGAPA-UNAM Project 104289 (ILG) and by the Office of Basic Energy Sciences, Division of Chemical Science, US-DOE under contract number W-31-109-ENG-38 (JJ). We thank the supercomputing time provided by DGSCA-UNAM.

References

1. See, for example, *Physics and Chemistry of Small Clusters*, P. Jena, B. K. Rao, and S. N. Khanna, Eds., Plenum Press: New York, 1987; Adv. Chem. Phys., I. Prigogine and S. A. Rice, Eds., 10, Part 2, Wiley-Interscience: New York, 1988; *Elemental and Molecular Clusters*, G. Benedek, T. P. Martin, and G. Pacchioni, Eds., Springer: Berlin, 1988; and references therein.
2. See, for example, Ph. Buffat and J. P. Borel, Phys. Rev. A 13, 2287 (1976); J. P. Borel, Surf. Sci. 106, 1 (1981); S. Iyima and T. Ichihashi, Phys. Rev. Lett. 56, 616 (1986); D. J. Smith, A. K. Petford-Long, R. L. Wallenberg, and J.-O. Bovin, Science 233, 872 (1986); P. M. Ajayan and L. D. Marks, Phys. Rev. Lett. 60, 585 (1988); T. Castro, R. Reifenberger, E. Choi and R. P. Andres, Phys. Rev. B 42, 8568 (1990); M. E. Lin, A. Ramachandra, R. P. Andres and R. Reifenberger, this volume; and references therein.
3. S. Sawada and S. Sugano, Z. Phys. D 14, 247 (1989).
4. F. Ercolessi, W. Andreoni, and E. Tossatti, Phys. Rev. Lett. 66, 911 (1991).
5. H.-P. Cheng and R. S. Berry, Mat. Res. Soc. Symp. Proc. 205, 241 (1991).
6. J. Jellinek and I. L. Garzon, Z. Phys. D. 20, 239 (1991).
7. I. L. Garzon and J. Jellinek, Z. Phys. D 20, 235 (1991)
8. Z. B.Güvenç, J. Jellinek and A. F. Voter, this volume.
9. L. Verlet, Phys. Rev. 159, 98 (1967).
10. I. Z. Fisher, *Statistical Theory of Liquids*, University of Chicago: Chicago, 1966.
11. J. Jellinek, unpublished results.

END

DATE
FILMED
3/11/92